An Improved Flow-Through Photocatalysis Device for the Removal of Emerging Contaminants

Ron Schweitzer , Soliman Khatib , Lior Levy , Giora Rytwo *

Article

An Improved Flow-Through Photocatalysis Device for the Removal of Emerging Contaminants

Ron Schweitzer [1], Soliman Khatib [1,2], Lior Levy [2] and Giora Rytwo [2,3,*]

[1] Dept. of Biotechnology, Tel Hai College, Israel

[2] MIGAL-Galilee Research Institute, Kiryat Shmona, Israel

[3] Depts. of Environmental Sciences & Water Sciences, Tel Hai College, Israel

[*] Correspondence: rytwo@telhai.ac.il or giorarytwo@gmail.com

Abstract

Cost-effective procedures usually can't achieve complete removal of priority contaminants present in water at very low concentrations (as pesticides or pharmaceuticals). Advanced oxidation processes (AOPs) represent promising technologies for removing priority contaminants from water at trace concentrations, yet practical implementation remains limited due to technical and economic constraints. This study presents an innovative flow-through photocatalytic device designed to overcome current limitations while achieving efficient contaminant removal at industrial scale. The device is integrates a UVC 254nm lamp-equipped flow chamber with automated dosing pumps for hydrogen peroxide and/or solid catalyst suspensions, coupled with a 30 nm pores membrane filtration system for catalyst recirculation. This configuration optimizes light-catalyst-pollutant contact while enabling combined catalytic processes. Performance evaluation using acesulfame (ACE) and iohexol (IHX) as model contaminants demonstrated rapid and effective removal. IHX degradation with UVC and 75 μM H_2O_2 achieved complete removal with $t_{95}\% = 7.23\pm1.21$ minutes (pseudo-order 0.25, $t_{1/2} = 3.27\pm0.39$ min), while ACE photolysis (with UVC only) required $t_{95}\% = 14.88\pm2.02$ minutes (pseudo-order 1.27, $t_{1/2} = 2.35\pm0.84$ min). The introduction of $t_{95}\%$ as a performance metric provides practical insights for near-complete contaminant removal requirements. Real-world efficacy was confirmed using tertiary wastewater treatment plant effluents containing 14 μg/L IHX, achieving complete removal within 8 minutes. However, carbamazepine degradation proved slower ($t_{95}\% > 74$ hours), highlighting the need for combined catalytic approaches for recalcitrant compounds. Spiking experiments (1000 μg/L) revealed concentration-dependent kinetics and synergistic effects between co-present contaminants. Analysis identified degradation byproducts consistent with previous studies, including tri-deiodinated iohexol (474.17 Da) intermediates. This scalable system, constructed from commercially available components, demonstrates potential for cost-effective industrial implementation. The modular design allows adaptation to various contaminants through adjustable AOP combinations (UV/H_2O_2, photocatalysts, ozone), representing a practical advancement toward addressing the gap between laboratory-scale photocatalytic research and full-scale water treatment applications.

Keywords: advanced oxidation process; photocatalysis; hydrogen peroxide; priority pollutants; iohexol; acesulfame; wastewater treatment plant

1. Introduction

The terms "priority pollutants" or "contaminants of concern" (CECs) are defined broadly and vary by source. The 1976 EPA Clean Water Act focuses specifically on 13 metals (including arsenic, cadmium, mercury, etc.) and 114 organic compounds [1]. Other definitions extend to any potentially hazardous substance detected in the environment—such as personal care products and pharmaceuticals—that may pose significant risks to human health and ecosystems [2,3]. Consequently, a wide spectrum of such pollutants has been identified in surface and groundwater,

including pesticides; pharmaceuticals (e.g., iodinated X-ray contrast agents); lifestyle and personal care compounds (such as caffeine and nicotine); industrial and water-treatment by-products; food additives (e.g., parabens, artificial sweeteners); flame retardants; and emerging nanomaterials (e.g., quantum dots, dendrimers, nanocomposites) [4].

Over the past few years, several reviews have summarized methods for the efficient removal of these contaminants. Some compare a variety of techniques across different approaches [5–8], while others examine specific processes. These include biological treatments—such as membrane bioreactors [9], specialized hydrogels[10], adsorption on tailored sorbents[11–14], and advanced oxidation processes (AOPs) [15–17]. For example, Rathi et al. [8] provide a detailed list of sorbents matched to specific trace pollutants and also discuss membrane separations and constructed wetlands. They conclude that hybrid strategies—combining techniques such as ultrafiltration, activated carbon adsorption, and ultrasonic irradiation[18]—can overcome the limitations of individual methods, noting that "emerging contaminants cannot be effectively treated by traditional wastewater treatment methods" and thus require supplementary treatments.

Advanced oxidation processes themselves are commonly classified in two ways: as chemical versus photochemical, depending on whether light is employed[17]; and as homogeneous versus heterogeneous, based on whether the oxidant is dissolved or solid[19]. All AOPs share the principle of in situ generation of reactive oxygen species (ROS) capable of degrading dissolved pollutants[20]. Typical ROS include hydroxyl, hydroperoxyl, and superoxide radicals[21–23]. The ultimate goal is the complete mineralization of toxins, emerging contaminants, pesticides, and other priority pollutants[24].

It is nearly impossible to capture in a single paper the vast body of AOP research published to date. Since 2004, the number of AOP–focused publications has grown by over thirteen-fold[25–28]. Roughly 23 % of these studies investigate heterogeneous photocatalysis—primarily TiO_2-based systems—while about 12 % explore direct photolysis or combined UV/H_2O_2 processes. Most laboratory studies employ batch-mode reactors or recirculating flow setups in which the effluent repeatedly passes through the catalyst or reactive membrane[29,30]. This arrangement simplifies operation, allows clear separation of treated and untreated streams for performance monitoring, and enables easy recovery of solid catalysts (e.g., by centrifugation). For practical, full-scale deployment, however, systems must operate in true continuous, flow-through mode—purifying contaminated water as it passes through—rather than relying on repeated batch or recirculation cycles. Continuous flow-through designs are essential to meet real-world treatment demands.

Despite extensive research on AOP methods, an AI-based search conducted in August 2025 found only about 500 commercial installations worldwide, most of which employ ozone or UV disinfection systems[31]. Key challenges and limitations include high capital and operational costs; process complexity and selectivity; sludge and residue generation; and sensitivity to operational parameters such as pH, temperature, and reactant concentration[32]. Additional hurdles arise from reduced performance in complex natural water matrices, difficulties in recovering catalysts from slurry reactors, and mass-transfer limitations in immobilized photocatalyst membranes[33]. Consequently, although hundreds of laboratory-scale studies report successful photocatalytic water-treatment devices, only a few have been scaled up commercially[34]—examples include the Purifics Photo-Cat system[35] or TrojanUVPhox 72AL75 reactor [36].

In a previous study, we described a laboratory-scale, slurry-type continuous-flow device for the photocatalytic degradation of priority pollutants[37,38]. The reactor was loaded with either synthetic hectorite (SHCa-1) or catalytic-grade TiO_2 nanoparticles and challenged with representative dyes, phenols, and pharmaceutical compounds. Under these controlled, synthetic-water conditions, the system achieved efficient degradation performance. However, all experiments to date were conducted in idealized matrices using relatively high pollutant concentrations (>1000 µg L^{-1}). Real-world water sources—often bearing complex chemistries and ultralow contaminant levels—remain untested, leaving most studies' practical applicability uncertain.

The device described in this study was evaluated for the degradation of two contaminants of emerging concern (CECs). Acesulfame potassium (Potassium 6-methyl-2,2-dioxo-2H-1,2λ^6,3-oxathiazin-4-olate, ACE; Figure 1) is an artificial sweetener employed as a sewer tracer in aquatic environments, since it is only partially removed by conventional wastewater treatment plants (WWTPs)[39,40]. Iohexol (5-[N-(2,3-dihydroxypropyl)acetamido]-2,4,6-triiodo-N,N'-bis(2,3-dihydroxypropyl)isophthalamide, IHX; Figure 1) is a non-biodegradable iodinated X-ray contrast agent detected at relatively high concentrations in water bodies worldwide[41–43]. Although both compounds' degradation by advanced oxidation processes (AOPs) has been studied in batch experiments[39,41,44,45], there are no reports of their treatment in continuous-flow systems.
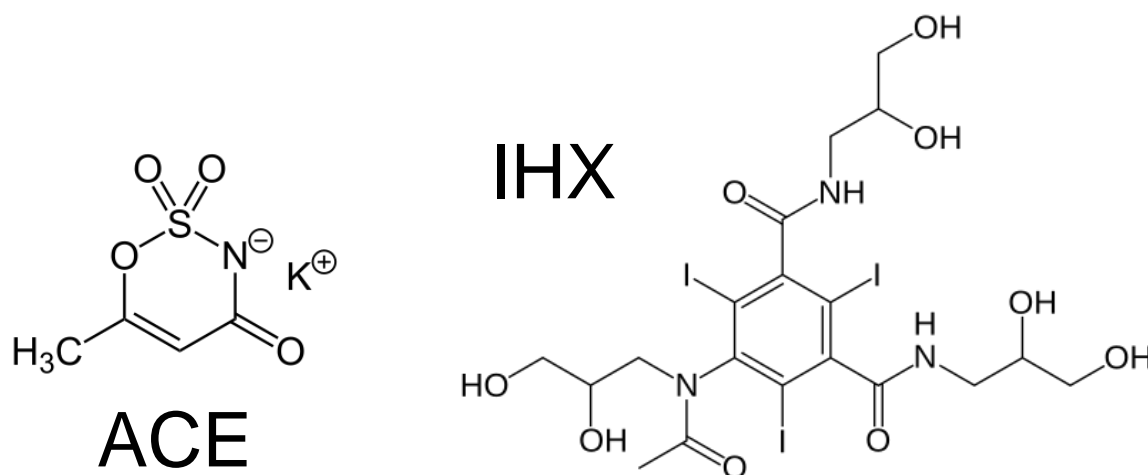
**Figure 1.** Acesulfame (ACE) and iohexol (IHX) chemical structure.

In this work, we present an upscaled reactor that integrates multiple AOP modalities—including a slurry-phase nano-photocatalyst, ozone, and hydrogen peroxide—with UV irradiation. This study focuses on the UVC only, and UVC/H$_2$O$_2$ configuration and assesses its efficacy for the complete removal of low concentrations of acesulfame and iohexol in tertiary effluent from a large WWTP.

2. Results

2.1. Flow Through Device for Photocatalytic Degradation

Figures 2 and 3 present a schematic diagram and a photographic image of the photocatalytic degradation device developed for this project. A brief video (Video S1), demonstrating the device in operation, is available in the Supplementary Material. A detailed description of the individual modules is provided in Section 4.1.
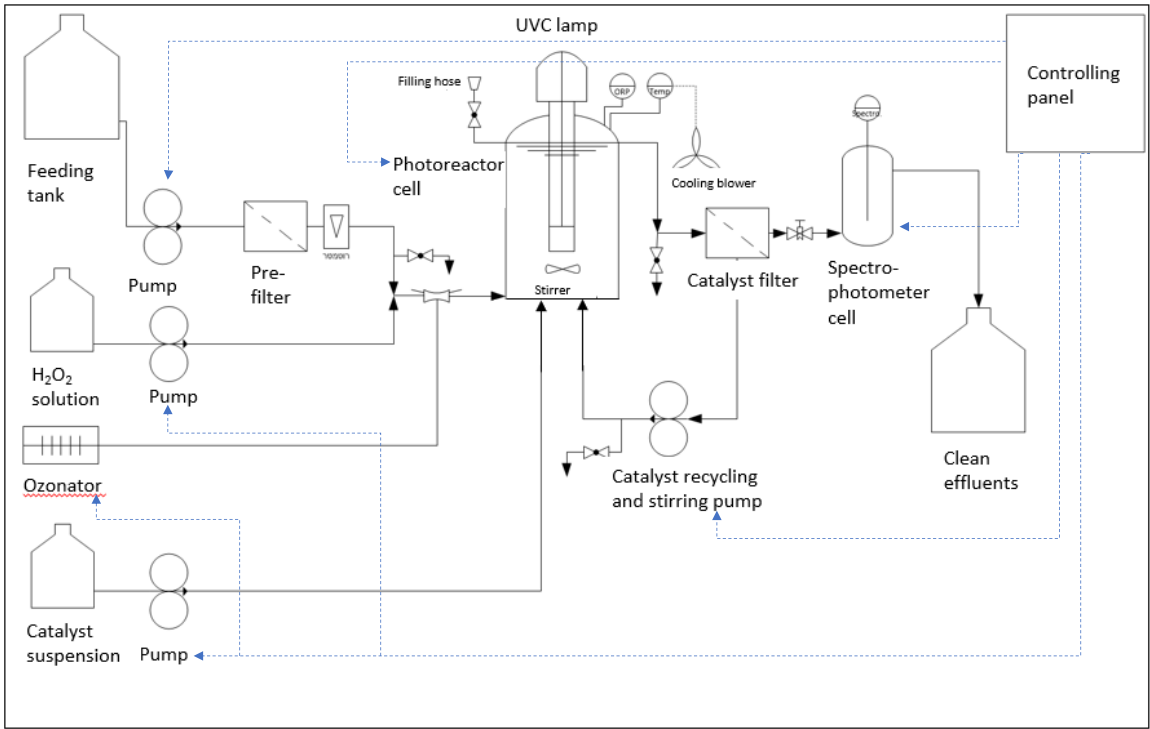
Figure 2. Schematic view of the photocatalytic degradation device. Solid and dashed lines indicate pipes and controlling cables, respectively (additional details in Section 4.1).
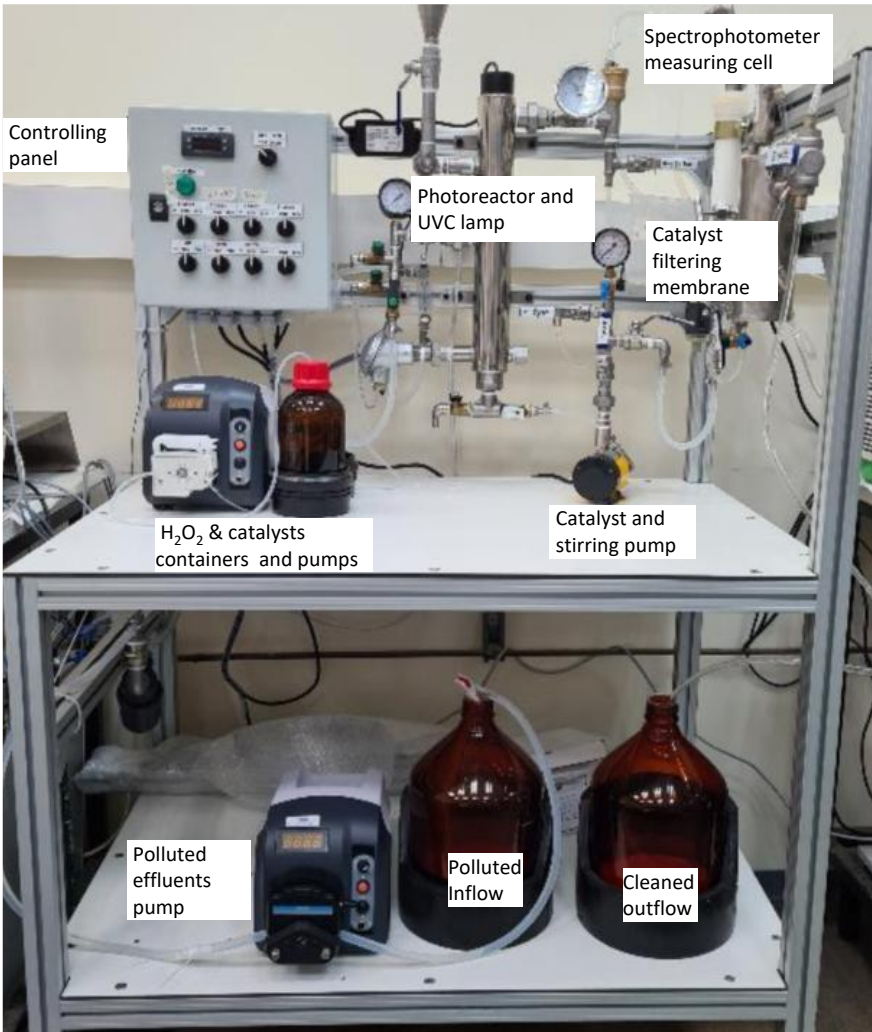
**Figure 3.** Picture of the photocatalytic degradation device.

2.2. Preliminary Experiments

As outlined in Section 4.2.1, solutions containing 0.5 mg L^{-1} of ACE or IHX were allowed to flow at a rate of 2.7 L h^{-1} without activating the UVC system or introducing any additional reagents. This was done to verify that no significant loss of pollutants occurred due to adsorption onto pipes, filter membranes, or other components of the device. The results, presented in Figure S1 of the Supplementary Material, show that within the first minute, there was a sharp decline in the measured concentrations of both ACE and IHX (C/C$_0$ values of 0.62 and 0.70, respectively). However, after 8 minutes, the concentrations increased substantially (C/C$_0$ values of 0.76 and 0.92 for ACE and IHX, respectively), and by 20 minutes, the system had reached equilibrium with C/C$_0$ values approaching 1.0.

2.3. Photodegradation Experiments in Synthetic Effluents

A detailed description of the procedure is provided in Section 4.2.2. Preliminary batch experiment performed in a 100-mLUV-C-transparent quartz glass (refractive Index n= 1.5048), 5.3-cm diameter beaker placed in a Rayonet RMR-600 mini photochemical chamber reactor (Southern New England Ultraviolet Company, Branford, Connecticut, USA), equipped with eight RMR 2537A lamps (254 nmwavelength), each lamp emitting an irradiance flux of 19 J m^{-2} s^{-1} at 254 nm (results not shown), that UVC light without any additional reagent yields photolysis of ACE, whereas degradation of IHX, requires addition H$_2$O$_2$. Similar results were reported in previous studies[46,47].

Figure 4 illustrates the photodegradation of ACE (without H$_2$O$_2$) and IHX (with H$_2$O$_2$ addition). Data points represent measured values (standard deviations from replicate experiments), and lines correspond to fits based on the pseudo-order kinetic model[48], briefly described in Section 4.2.2. Complete degradation of IHX was achieved after approximately 8 min, with a pseudo-order of 0.25 and a half-life (t$_{1/2}$) of 3.27 ± 0.39 min. ACE reached near-complete degradation after approximately 20 min, with a pseudo-order of 1.27 and a half-life of 2.35 ± 0.84 min. Because regulatory focus on priority trace pollutants emphasizes near-total removal, we define the time to 95% degradation (t$_{95}$%) as denoted in Equation (4). For IHX, t$_{95}$% is 7.23 ± 1.21 min, whereas for ACE, t$_{95}$% is 14.88 ± 2.02 min. It should be noted that IHX degradation involved H$_2$O$_2$ injection, while ACE underwent direct photolysis without additional reagents or catalysts. The agreement between measured data and model predictions is excellent, with R^2 = 0.989 for both ACE and IHX.
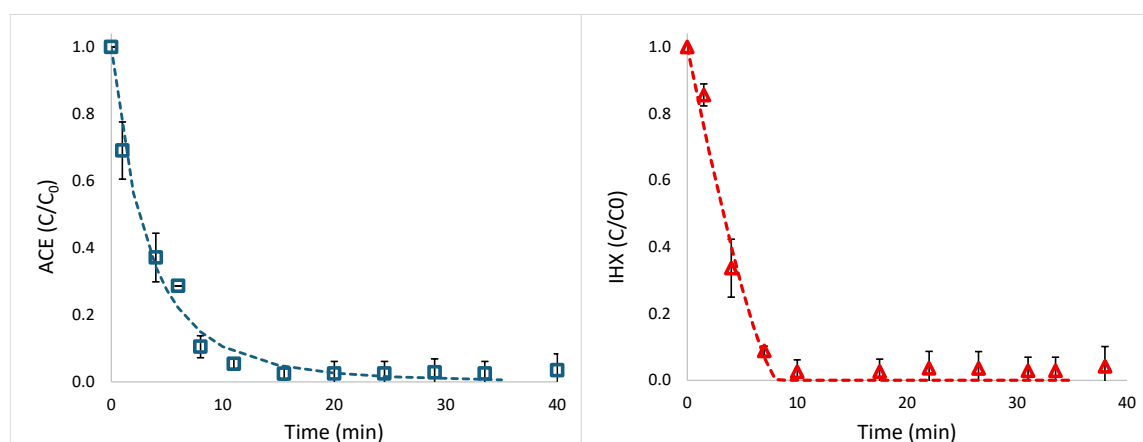
Figure 4. Average photolysis of acesulfame (ACE, left panel) and photodegradation of iohexol (IHX, right panel) with injection of 75 μM (2.55 mg L^{-1}) H$_2$O$_2$. Points indicate measured values with standard error. Lines indicate evaluated values based on the "pseudo-order method". Pollutants concentrations ranged between 0.1-0.5 mg L^{-1}.

2.4. Photodegradation Experiments in Shafdan WWTP Effluents

2.4.1. Degradation of Pollutants on Tertiary Treatment Effluents

The first experiment was conducted on tertiary-treatment effluents from Israel's largest wastewater-treatment plant, prior to disinfection and chlorination, with the addition of 75 μM H_2O_2, as described in Section 4.2.3. The initial iohexol (IHX) concentration in the effluents was 14 μg L^{-1}, whereas acesulfame (ACE) was below the LC-MS detection limit. A significant trace concentration of carbamazepine (CBZ)—an antiepileptic drug frequently detected in WWTP effluents[49]—was also present. Although this study focused on ACE and IHX, we also monitored CBZ degradation in the real-world effluents. Figure 5 shows that IHX degradation is very rapid, reaching complete removal within 8 min, while CBZ degrades much more slowly. Previous UVC/H_2O_2 studies report efficient CBZ removal[49,50], but they employed H_2O_2 concentrations 50–100 times higher (5 000–20 000 μM) than those used here.

Under our conditions, using the pseudo-order kinetic model yields a reaction order of 2.84 for CBZ, a half-life ($t_{1/2}$) of 26.5 min, and t_{95}% of 4 484 min (> 74 h). Given that most rapid AOPs for CBZ employ heterogeneous catalysts[51,52], such slow removal under low-H_2O_2 UVC photolysis is unsurprising.

While exact kinetics depend on system parameters—including UVC intensity—previous work shows that combining low H_2O_2 doses with mineral catalysts (e.g., TiO_2 or clay minerals) can reduce CBZ half-life to under 6 min[12].
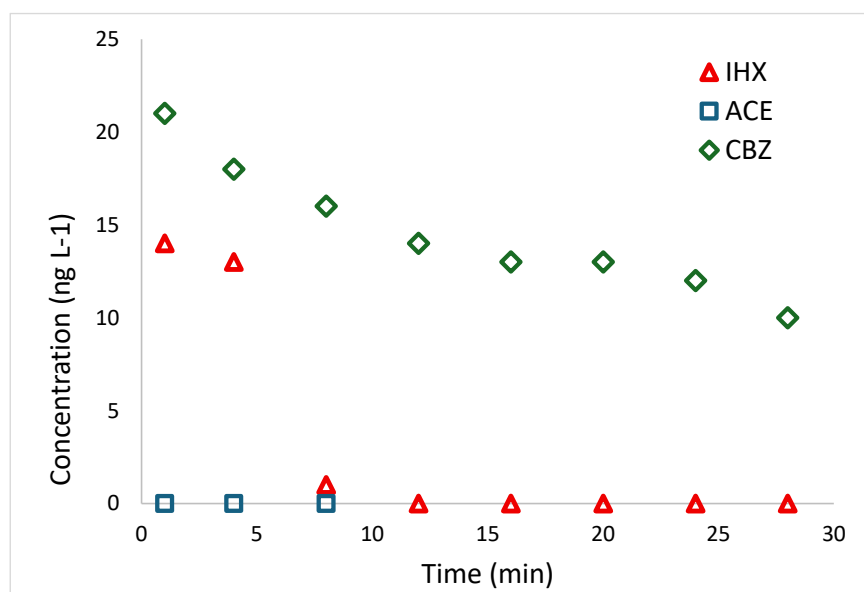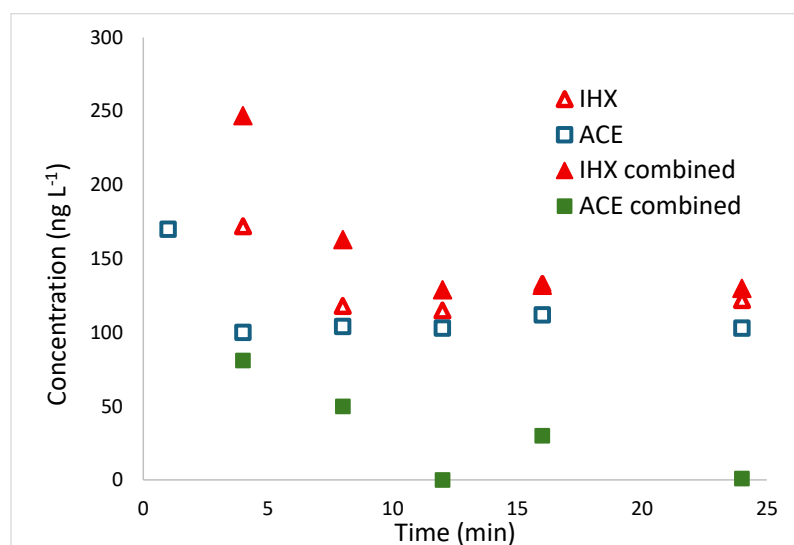

Figure 5. Photodegradation of iohexol (IHX) and carbamazepine (CBZ) in Shafdan WWTP tertiary effluent, carried out with the addition of 75 μM (2.55 mg L^{-1}) H_2O_2. Acesulfame (ACE) was not detected in the effluent.

2.4.2. Degradation on Tertiary Treatment Effluents with IHX and ACE Spiking

To evaluate the device's performance under high pollutant loads representative of industrial discharges in real effluent, Shafdan WWTP tertiary effluent was spiked with 1000 μg L^{-1} of ACE and IHX, both individually and in combination. Figure 6 presents the results of these spiking experiments, as detailed in Section 4.2.3.

To enhance clarity in Figure 6, the y-axis excludes the initial 1000 μg L^{-1} concentration for all samples, zooming in on the degradation dynamics. Iohexol (IHX) shows nearly identical decay profiles whether tested alone or with acesulfame (ACE), leveling off at about 130 μg L^{-1} even after 25 minutes, so complete removal isn't achieved. ACE alone degrades at a comparable pace, but when combined with IHX it disappears entirely within 12 minutes. This suggests that pollutants'

interactions can accelerate the breakdown of the more labile compounds. The persistent IHX residue implies the process follows higher-order kinetics, which tend to be effective at high pollutant loads but less so at lower concentrations[48].
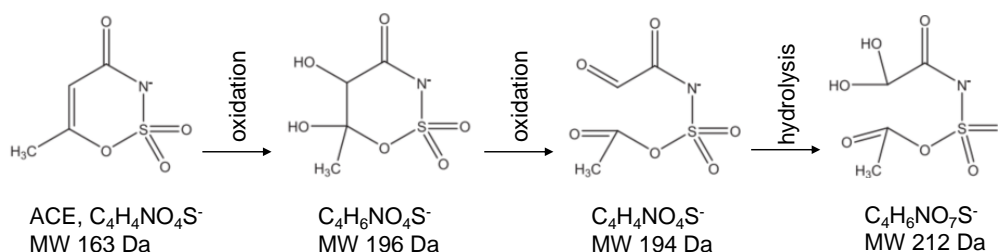

Figure 6. Photodegradation of iohexol (IHX) and acesulfame (ACE) from Shafdan WWTP spiked with 1000 µg L^{-1} of pollutants, when added separately (ACE, IHX) or together ("combined" samples).

2.5. Suggested Photodegradation By-Products

The workflow for detecting and tracking photodegradation by-products is outlined in Section 4.3.2. Our LC-MS/MS method was optimized for quantifying the parent contaminants (ACE and IHX), so untargeted screening revealed only one plausible intermediate per compound—and those appeared within the first 4 minutes of irradiation.

2.5.1. ACE Screened Photodegradation By-Products

Compound Discoverer 3.1 (Thermo Xcalibur v3.3.0.305) flagged two intermediate species for ACE at 194 Da and 212 Da. Although UV-AOP studies including direct solar [53] or LED-UVC photolysis at different wavelengths [44], UV/persulfate [45] and UV/hydrogen peroxide[44,54]—have proposed by-products in the 148.9–222.2 Da range, our untargeted LC-MS/MS screen only confirmed the 194 Da and 212 Da species. Xue et al. also identified these two: the 194 Da product forms after two successive oxidations (see Figure 7), and the 212 Da compound arises following an additional hydrolysis step.

**Figure 7.** Photodegradation suggested path for screened byproducts of acesulfame (ACE).

2.5.2. IHX Screened Photodegradation By-Products

The degradation of iohexol (IHX) by various AOPs has been extensively investigated. Zilberman et al. [55] found ozonation to be inefficient, achieving only partial IHX removal; the resulting by-products exhibited persistence, stability, and toxicity profiles similar to the parent compound, with

some even more toxic than IHX itself. Electro-enhanced activation promotes deiodination, amide hydrolysis, C–OH oxidation, hydroxyl addition, hydrogen abstraction, and elimination reactions, yet most by-products produced under these conditions showed low toxicity toward fish, daphnia, and algae[56]. Hu et al.[57] detailed the kinetics of UV-induced IHX oxidation but noted an increase in the toxic by-product iodoform (CHI_3) during the process. A recent study that tested LED UV photodegradation at different wavelengths detected seven different transformation products and concluded that "overall toxicity increased after UV-LED photolysis, posing a considerable risk that requires careful attention" [58].

Under UV/H_2O_2 treatment—analogous to the conditions in our device—Giannakis et al. [41] identified 13 IHX by-products (ranging 444–712 Da) after 5 min of irradiation, whereas only three by products (514–653 Da) persisted after 15 min. Our LC-MS/MS analysis confirms the formation of a tri-deiodinated iohexol intermediate ($C_{19}H_{27}N_3O_{11}$, m/z 474.1726), in which the 2,4,6-triiodophenyl ring is converted to a hydroxylated benzene core while retaining the acetamido side chains (Figure 8). This structure corresponds to one of the by-products proposed by Giannakis et al. that is present both after 5 min and 15 min UV/H_2O_2 treatments. A detailed suggested degradation pathway that forms such component built with the help of Microsoft Copilot AI (Microsoft, 2025) is provided as Scheme S1 in the Supplementary Material.
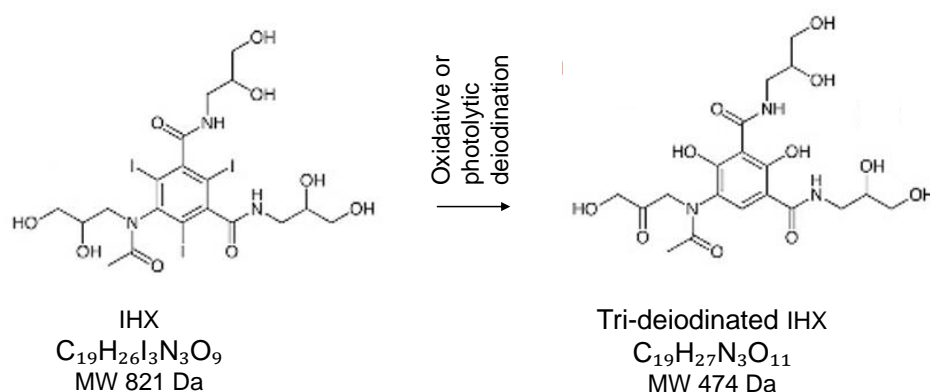
Figure 8. Photodegradation byproducts of iohexol (IHX).

3. Discussion

The flow-through photocatalytic device demonstrated rapid and near-complete removal of low-concentration iohexol (IHX) and acesulfame (ACE) under UVC/H_2O_2 and UVC-only conditions, respectively. The UV/H_2O_2 configuration achieved complete IHX degradation within 8 min ($t_{95}\%$ = 7.23 ± 1.21 min), confirming the device's ability to generate sufficient reactive oxygen species for halogenated compounds. ACE photolysis required longer exposure ($t_{95}\%$ = 14.88 ± 2.02 min) but proceeded efficiently without added reagents, highlighting UVC direct photolysis as a viable route for certain trace pollutants.

Spiking experiments at 1 000 µg L^{-1} concentrations revealed concentration-dependent kinetics and pollutant interactions. Iohexol remained at ~130 µg L^{-1} after 25 min, whether alone or mixed with ACE, indicating higher-order kinetics that slow at lower residual levels. In contrast, ACE spiked alone followed similar decay to IHX alone, but its combined sample with IHX achieved full removal within 12 min—suggesting that co-contaminant interactions can accelerate degradation of the more labile species.

Real-world effluent trials underscored the system's promise and its current limits. Using tertiary wastewater from Shafdan WWTP, IHX was eliminated within 8 min, mirroring synthetic results despite complex water matrices. Carbamazepine (CBZ), however, displayed sluggish kinetics ($t_{95}\%$ > 74 h) under low H_2O_2 dosing, underscoring the need for heterogeneous catalysts or higher oxidant loads to tackle recalcitrant pharmaceuticals.

By-product screening confirmed known intermediates without revealing novel species. Acesulfame intermediates at 194 Da and 212 Da aligned with previous UV/AOP studies, while a tri-deiodinated iohexol (m/z 474.17) matched reported UV/H_2O_2 pathways. The absence of additional by-products in early irradiation stages suggests that extended treatment or catalytic enhancements may be required for full mineralization. More extensive detailed LC-MS /MS measurements are required to determine if toxic degradation byproducts remain after the process, as was reported in several prior studies. Additional experiments based on flow through devices should be performed to test such persistent priority pollutants, at a relevant range of concentrations and conditions that fit real-world situations, by employing other AOP agents, such as TiO_2 or similar solid catalysts, to exploit the combination of homo- and heterogeneous catalytic processes.

4. Materials and Methods

4.1. Description of the Device

The slurry-type continuous-flow device for photocatalytic degradation of priority pollutants (Figure 2) is an upscale of a previously reported laboratory-scale system[37,38]. Its core is the photoreactor module (denoted "photoreactor cell" or "photoreactor and UVC lamp" in Figures 2 and 3), which integrates an AMD-UV-21 disinfection unit (Zalion Ltd., Bat Yam, Israel). This module houses a 21 W UVC lamp (254 nm) providing an irradiance of 15.2 mW cm^{-2} and supports a nominal flow rate up to 13.6 L h^{-1}. Contaminated effluent is drawn from the feeding tank by a PP-X-575 peristaltic pump (MRC Laboratory Instruments, Holon, Israel) fitted with a YZ1515X head and S-18 tubing, delivering up to 35 L h^{-1}[59]. Hydrogen peroxide and heterogeneous catalyst suspensions are dosed directly into the photoreactor via two independent PP-X-576 peristaltic pumps (300–3 000 mL h^{-1} each), which may operate separately or in tandem. An optional ozonator can also be integrated. Downstream of the photoreactor, treated effluent passes through a 2 m² polysulfone NUF® membrane (NUF Filtration, Caesarea, Israel) rated for 150 L h^{-1} and an absolute pore size of 30 nm ("catalyst filter," Figure 2). Originally developed for hemodialysis[60], this membrane permits continuous recirculation of solid catalysts to the photoreactor ("catalyst recycling and stirring pump" in Figure 3) via an NH-1PX-Z magnetic-drive centrifugal pump (March May Ltd., Cambridgeshire, UK), and the transmembrane pressure (TMP) used was between 0.6-1.0 bar. Finally, the clarified effluent flows through a DP400 dip-probe cuvette connected to a Black Comet SR spectrophotometer (SpectraWiz software; StellarNet Inc., Tampa, FL, USA), enabling real-time UV–Vis monitoring. All modules—including the main feed pump, H_2O_2 and catalyst dosing pumps, optional ozonator, UVC photoreactor, membrane filtration and recycling system, and spectrophotometer monitoring cell—are controlled from a central panel to ensure full operational flexibility.

4.2. ACE and IHX Photodegradation Experiments

Analytical ACE, IHX, and a 30% (9.79 M) concentrated H_2O_2 solution were obtained from Merck/Sigma-Aldrich (Merck KGaA, Darmstadt, Germany). Stock solutions of 1 mg L^{-1} of both pollutants were prepared and kept in dark large bottles at room temperature (23±1C$^\circ$). Experiments were performed by pumping pollutants at concentrations ranging between 0.15-0.5 mg L^{-1} at 25 RPM (equivalent to a rate flow of 2.27 L h^{-1}).

4.2.1. Preliminary Evaluation and Maintenance of the System

To avoid biases caused by potential adsorption of pollutants onto the pipes and membranes, a preliminary assessment of the system's performance was conducted by running a 0.5 mg L^{-1} solution of each pollutant through the setup without activating the UVC lamp or adding any reagents. The results are presented in Section 2.2.

Since previously used pollutants in the system may leave residues that could affect subsequent measurements, the system was cleaned after each run with 1 L of 5% ethanol in distilled water,

followed by 2 L of distilled water. At the end of the process, the effluent was tested using the spectrophotometer monitoring device described in Section 4.1, and the first sample in the subsequent LC-MS/MS analysis confirmed that no residues of the previous pollutants remained.

4.2.2. Photodegradation Experiments in Synthetic Effluents

Based on preliminary experiments and literature indicating that ACE undergoes photolysis under UVC radiation without the need for additional reagents[44], experiments involving ACE did not include the addition of H_2O_2. In contrast, experiments with IHX involved the injection of H_2O_2 to achieve an inflow concentration of 75 μM (2.55 mg L^{-1}). Concentrations of pollutants in the outflow were measured using HPLC, and samples were additionally analyzed by LC-MS/MS to suggest and monitor potential degradation by-products. The measured concentrations of remaining pollutants were evaluated as relative residual concentrations (C/C_0), and the average was calculated across three independent experiments. To assess process efficiency, half-life times ($t_{1/2}$) and the time required to achieve 95% degradation ($t_{95\%}$) were determined using the "pseudo-order method" extensively described by Rytwo and Zelkind[48]. Briefly, pseudo-order kinetic models are based on the integration of the simplified rate law[61,62]:

$$v = \frac{d[A]}{dt} = -k_a[A]^{n_a} \tag{1}$$

where v is the reaction rate, k_a is the apparent rate coefficient, and n_a is the apparent or "pseudo" reaction order. Simple integration of Equation (1) (as long as $n_a \neq 1$) yields:

$$\text{for } n_a \neq 1: \ [A]_{(t)} = \left(\frac{1}{\frac{1}{[A_0]^{n_a-1}} + (n_a-1)k_a t} \right)^{\frac{1}{n_a-1}} \tag{2}$$

To relatively objectively compare efficiency of processes, "half-life time" ($t_{1/2}$) can be calculated by solving Equations (2) for the case where the concentration is half of its initial value, thus $[A]_{(t)} = 0.5$, yielding:

$$\text{for } n_a \neq 1: \ t_{1/2} = \frac{2^{n_a-1}-1}{(n_a-1)k_a[A_0]^{n_a-1}} \tag{3}$$

Considering that in priority trace pollutants the goal is almost complete removal, it worth defining the evaluated time until 95% of the pollutant is removed ($t_{95\%}$), as:

$$\text{for } n_a \neq 1: \ t_{95\%} = \frac{(\frac{1}{0.05})^{n_a-1}-1}{(n_a-1)k_a[A_0]^{n_a-1}} \tag{4}$$

Specific adaptation to Equations (2) and (3) for pseudo-*first*-order ($n_a = 1$) [63] yields:

$$\text{for } n_a = 1: \ [A]_{(t)} = [A]_0 e^{-k_a t} \text{ and } t_{1/2, n=1} = \frac{\ln(2)}{k_a} \tag{5}$$

Estimates of the best-fit pseudo-order (n), and the rate constant (k_a) are made by minimizing the overall root mean square error (RMSE)[48]. The procedure can be easily performed using the "Solver" add-on in Excel® software. Following that, $t_{1/2}$ and $t_{95\%}$ can be evaluated based on n and k_a. These calculations enable comparison between different processes without requiring an *a priori* assumption about the reaction's kinetic order, thus providing a relatively objective evaluation of the process's efficiency by identifying the pseudo-order and corresponding degradation times. [64,65].

4.2.3. Photodegradation Experiments on Shadan WWTP Tertiary Effluents

To evaluate the effectiveness of ACE and IHX degradation in real effluents, water from Shafdan WWTP [66] after tertiary treatment, but before chlorination were brought to the laboratory. A full description of the WTTP and the methods adopted in the establishment can be found in previous reports[67]. The pH was 7.55 and turbidity < 4 NTU. Such values are similar to those reported for Shafdan effluent in the literature[68]. Preliminary LC-MS screening measurements for priority

pollutants indicated that the effluents contained 14 µg L^{-1} IHX and 22 µg L^{-1} carbamazepine (CBZ), but no ACE. Three different experiments were performed, all of them with injection of 75 µM (2.55 mg L^{-1}) of H$_2$O$_2$ (a) Shafdan original effluents (b) Shafdan original effluents spiked with 1000 µg L^{-1} of ACE or IHX in separate experiments, and (c) Shafdan original effluents spiked with 1000 µg L^{-1} of both ACE and IHX.

4.3.1. HPLC Measurements

Part of the measurements were performed by injecting 5 µL of the extracted solutions into a UHPLC connected to a photodiode array detector (Dionex Ultimate 3000), with a reverse-phase column (ZORBAX Eclipse plus C18, 3.0*100 mm, 1.8 µm). The mobile phase consisted of (A) DDW with 0.1% formic acid and (B) acetonitrile containing 0.1% formic acid. The gradient started with 2% B and kept isocratic for 2 min, then increased to 75% B in 16 minutes, then increased to 95% in 1 minute and kept isocratic at 95% B for 4 minutes. Phase B returned to 5% in 2 minutes and the column allowed to equilibrate at 5% B for 3 minutes before the next injection. The flow rate was 0.4 mL/min. Column temperature set to 35°C.

4.3.2. MS/MS Analysis

Measurements for analysis of degradation byproducts were made with Mass spectrometry (MS) analysis performed with Heated Electrospray ionization (HESI-II) source connected to a Q Exactive™ Plus Hybrid Quadrupole-Orbitrap™ Mass Spectrometer Thermo Scientific ™. ESI capillary voltage was set to 3900 V in positive mode and 3500 V in negative mode, capillary temperature to 350°C, gas temperature to 350°C. Sheath gas flow set to 35 ml/min, aux gas flow to 10 ml/min and sweep gas flow to 1 ml/min. The mass spectra in Positive-ion mode (m/z 67–900) and in Negative mode (m/z 50–300) and acquired with high resolution (FWHM=70,000 at m/z=200. For MS^2 analysis collision energy set to 20, 30 and 50 EV**.**

Data preprocessing for MS targeted analysis were conducted using Thermo Scientifc™ Xcalibur™ instrument control software. Extracted ion chromatograms for figure production were generated in Xcalibur 4.0.27.19 software using a mass window of (+/−) 5 ppm. Exact m/z values used for figure creation and peak integration corresponded to theoretical [M + H]+ ion m/z values and were as follows: Iohexol 821.8876 m/z, [M - H] Acesulfame 161.9866 m/z. Peak integration was performed using QN™ software after determine LOD, LOQ and linearity for each analyte

Data preprocessing for MSMS untargeted analysis and peak determination and peak area integration for IHX and ACE decomposition products, was performed with Compound Discoverer 3.1 (Thermo Xcalibur, Version 3.3.0.305) using metabolism workflow. Auto-integration was manually inspected and corrected if necessary. For some of the compounds, identification was performed based on MzCloud database using MS^2 data and ChemSpider database using MS^2 data and HRMS.

Conflicts of Interest: The authors declare no conflicts of interest. The funders had no role in the design of the study; in the collection, analyses, or interpretation of data; in the writing of the manuscript; or in the decision to publish the results.

Abbreviations

The following abbreviations are used in this manuscript:

ACE	Potassium 6-methyl-2,2-dioxo-2H-1,2λ^6,3-oxathiazin-4-olate- acesulfame
AOP	Advanced oxidation process
C/C_0	Ration between measured concentration and initial concentration
CBZ	Carbamazepine
EPA	US Environmental Protection Agency
H_2O_2	Hydrogen peroxide
IHX	5-[N-(2,3-Dihydroxypropyl)acetamido]-2,4,6-triiodo-N,N'-bis(2,3-dihydroxypropyl)isophthalamide, iohexol
min	Minutes
$t_{1/2}$	Half life time
$t_{95\%}$	Evaluated time for the degradation of 95% of a pollutant
TiO_2	Catalytic grade titanium dioxide
TMP	Trans-membrane pressure
UV	Ultraviolet light
UVC	Ultraviolet light in the range 190-280 nm
WWTP	Wastewater treatment plant

References

1. EPA Toxic and Priority Pollutants Under the Clean Water Act | US EPA Available online: https://www.epa.gov/eg/toxic-and-priority-pollutants-under-clean-water-act (accessed on 2 July 2025).

2. Sauvé, S.; Desrosiers, M. A Review of What Is an Emerging Contaminant. *Chem. Cent. J.* **2014**, *8*, 1–7, doi:10.1186/1752-153X-8-15/FIGURES/2.

3. Ramírez-Malule, H.; Quiñones-Murillo, D.H.; Manotas-Duque, D. Emerging Contaminants as Global Environmental Hazards. A Bibliometric Analysis. *Emerg. Contam.* **2020**, *6*, 179–193, doi:10.1016/J.EMCON.2020.05.001.

4. Naidu, R.; Arias Espana, V.A.; Liu, Y.; Jit, J. Emerging Contaminants in the Environment: Risk-Based Analysis for Better Management. *Chemosphere* **2016**, *154*, 350–357, doi:10.1016/J.CHEMOSPHERE.2016.03.068.

5. Kathi, S.; El Din Mahmoud, A. Trends in Effective Removal of Emerging Contaminants from Wastewater: A Comprehensive Review. *Desalin. Water Treat.* **2024**, *317*, 100258, doi:10.1016/J.DWT.2024.100258.

6. Morin-Crini, N.; Lichtfouse, E.; Fourmentin, M.; Ribeiro, A.R.L.; Noutsopoulos, C.; Mapelli, F.; Fenyvesi, É.; Vieira, M.G.A.; Picos-Corrales, L.A.; Moreno-Piraján, J.C.; et al. Removal of Emerging Contaminants from Wastewater Using Advanced Treatments. A Review. *Environ. Chem. Lett. 2022 202* **2022**, *20*, 1333–1375, doi:10.1007/S10311-021-01379-5.

7. Mahmood, T.; Momin, S.; Ali, R.; Naeem, A.; Khan, A.; Mahmood, T.; Momin, S.; Ali, R.; Naeem, A.; Khan, A. Technologies for Removal of Emerging Contaminants from Wastewater. *Wastewater Treat.* **2022**, doi:10.5772/INTECHOPEN.104466.

8. Rathi, B.S.; Kumar, P.S.; Show, P.L. A Review on Effective Removal of Emerging Contaminants from Aquatic Systems: Current Trends and Scope for Further Research. *J. Hazard. Mater.* **2021**, *409*, 124413, doi:10.1016/j.jhazmat.2020.124413.

9. Sengupta, A.; Jebur, M.; Kamaz, M.; Wickramasinghe, S.R. Removal of Emerging Contaminants from Wastewater Streams Using Membrane Bioreactors: A Review. *Membr. 2022, Vol. 12, Page 60* **2021**, *12*, 60, doi:10.3390/MEMBRANES12010060.

10. Sharma, K.; Choudhary, P.; Majeed, A.; Guleria, S.; Kumar, M.; Rana, A.K.; Rajauria, G. Cellulose Based Membranes, Hydrogels and Aerogels for Water Treatment Application. *Ind. Crops Prod.* **2025**, *225*, 120474, doi:10.1016/J.INDCROP.2025.120474.

11. Grassi, M.; Kaykioglu, G.; Belgiorno, V.; Lofrano, G. *Removal of Emerging Contaminants from Water and Wastewater by Adsorption Process*; Springer Netherlands, 2012; ISBN 9789400739161.

12. Levakov, I.; Shahar, Y.; Rytwo, G. Carbamazepine Removal by Clay-Based Materials Using Adsorption and Photodegradation. *Water (Switzerland)* **2022**, *14*, doi:10.3390/w14132047.

13. Aziz, A.; Al-Khatib, I.A.; Rahman, R.O.A.; Imai, T.; Hung, Y.-T.; Almeida-Naranjo, C.E.; Guerrero, V.H.; Alejandra Villamar-Ayala, C. Emerging Contaminants and Their Removal from Aqueous Media Using Conventional/Non-Conventional Adsorbents: A Glance at the Relationship between Materials, Processes, and Technologies. *Water 2023, Vol. 15, Page 1626* **2023**, *15*, 1626, doi:10.3390/W15081626.

14. Dai, C.F.; Khoruzhenko, O.; Zhang, C.; Zhu, Q.L.; Jiao, D.; Du, M.; Breu, J.; Zhao, P.; Zheng, Q.; Wu, Z.L. Magneto-Orientation of Magnetic Double Stacks for Patterned Anisotropic Hydrogels with Multiple Responses and Modulable Motions. *Angew. Chemie Int. Ed.* **2022**, *61*, e202207272, doi:10.1002/anie.202207272.

15. Zhang, Y.; Zhang, X.; Wang, S. Recent Advances in the Removal of Emerging Contaminants from Water by Novel Molecularly Imprinted Materials in Advanced Oxidation Processes—A Review. *Sci. Total Environ.* **2023**, *883*, 163702, doi:10.1016/J.SCITOTENV.2023.163702.

16. Demetriou Dionysiou, D.; Wang, Y.; Wang, H. Advanced Oxidation Processes for Emerging Contaminant Removal. *Adv. Oxid. Process. Emerg. Contam. Remov.* **2023**, 298, doi:10.3390/BOOKS978-3-0365-6610-8.

17. Wypart-Pawul, A.; Neczaj, E.; Grobelak, A. Advanced Oxidation Processes for Removal of Organic Micropollutants from Wastewater. *Desalin. Water Treat.* **2023**, *305*, 114–128, doi:10.5004/DWT.2023.29665.

18. Secondes, M.F.N.; Naddeo, V.; Belgiorno, V.; Ballesteros, F. Removal of Emerging Contaminants by Simultaneous Application of Membrane Ultrafiltration, Activated Carbon Adsorption, and Ultrasound Irradiation. *J. Hazard. Mater.* **2014**, *264*, 342–349, doi:10.1016/J.JHAZMAT.2013.11.039.

19. Poyatos, J.M.; Muñio, M.M.; Almecija, M.C.; Torres, J.C.; Hontoria, E.; Osorio, F. Advanced Oxidation Processes for Wastewater Treatment: State of the Art. *Water. Air. Soil Pollut.* **2010**, *205*, 187–204, doi:10.1007/s11270-009-0065-1.

20. Mazille, F.; Spuhler, D. Advanced Oxidation Processes Available online: https://sswm.info/sswm-university-course/module-6-disaster-situations-planning-and-preparedness/further-resources-0/advanced-oxidation-processes (accessed on 14 December 2021).

21. Ghime, D.; Ghosh, P.; Ghime, D.; Ghosh, P. Advanced Oxidation Processes: A Powerful Treatment Option for the Removal of Recalcitrant Organic Compounds. *Adv. Oxid. Process. - Appl. Trends, Prospect.* **2020**, doi:10.5772/INTECHOPEN.90192.

22. Comninellis, C.; Kapalka, A.; Malato, S.; Parsons, S.A.; Poulios, I.; Mantzavinos, D. Advanced Oxidation Processes for Water Treatment: Advances and Trends for R&D. *J. Chem. Technol. Biotechnol.* **2008**, *83*, 769–776, doi:https://doi.org/10.1002/jctb.1873.

23. Hübner, U.; Spahr, S.; Lutze, H.; Wieland, A.; Rüting, S.; Gernjak, W.; Wenk, J. Advanced Oxidation Processes for Water and Wastewater Treatment – Guidance for Systematic Future Research. *Heliyon* **2024**, *10*, e30402, doi:10.1016/J.HELIYON.2024.E30402.

24. O'Shea, K.E.; Dionysiou, D.D. Advanced Oxidation Processes for Water Treatment. *J. Phys. Chem. Lett.* **2012**, *3*, 2112–2113, doi:10.1021/JZ300929X.

25. Claude AI Advanced Oxidation Processes Publications Trends (2004-2024) | Claude | Claude Available online: https://claude.ai/public/artifacts/68bf09bc-f715-44d0-ae01-efeaf6784d7f (accessed on 2 August 2025).

26. Macías-Quiroga, I.F.; Henao-Aguirre, P.A.; Marín-Flórez, A.; Arredondo-López, S.M.; Sanabria-González, N.R. Bibliometric Analysis of Advanced Oxidation Processes (AOPs) in Wastewater Treatment: Global and Ibero-American Research Trends. *Environ. Sci. Pollut. Res.* **2021**, *28*, 23791–23811, doi:10.1007/S11356-020-11333-7/FIGURES/2.

27. Garrido-Cardenas, J.A.; Esteban-García, B.; Agüera, A.; Sánchez-Pérez, J.A.; Manzano-Agugliaro, F. Wastewater Treatment by Advanced Oxidation Process and Their Worldwide Research Trends. *Int. J. Environ. Res. Public Health* **2020**, *17*, doi:10.3390/ijerph17010170.

28. Clímaco Cunha, I.L.; Machado, P.G.; de Oliveira Ribeiro, C.; Kulay, L. Bibliometric Analysis of Advanced Oxidation Processes Studies with a Focus on Life Cycle Assessment and Costs. *Environ. Sci. Pollut. Res. 2024 3115* **2024**, *31*, 22319–22338, doi:10.1007/S11356-024-32558-W.

29. Almeida da Silva, T.C.; Marchiori, L.; Oliveira Mattos, B.; Ullah, S.; Barud, H. da S.; Romano Domeneguetti, R.; Rojas-Mantilla, H.D.; Boldrin Zanoni, M.V.; Rodrigues-Filho, U.P.; Ferreira-Neto, E.P.; et al. Designing Highly Photoactive Hybrid Aerogels for In-Flow Photocatalytic Contaminant Removal Using Silica-Coated Bacterial Nanocellulose Supports. *ACS Appl. Mater. Interfaces* **2023**, *15*, 23146–23159, doi:10.1021/ACSAMI.3C02008/SUPPL_FILE/AM3C02008_SI_001.PDF.

30. Vale, M.; Barrocas, B.T.; Serôdio, R.M.N.; Oliveira, M.C.; Lopes, J.M.; Marques, A.C. Robust Photocatalytic MICROSCAFS® with Interconnected Macropores for Sustainable Solar-Driven Water Purification. *Int. J. Mol. Sci.* **2024**, *25*, 5958, doi:10.3390/IJMS25115958/S1.

31. Veolia Disinfection & Oxidation Water Treatment: Ozone & UV Systems | Veolia Available online: https://www.watertechnologies.com/products/disinfection-oxidation (accessed on 2 August 2025).

32. Waterandwastewater.com Advanced Oxidation Processes in Wastewater Treatment: Efficiency and Innovation - Water & Wastewater Available online: https://www.waterandwastewater.com/advanced-oxidation-processes-in-wastewater-treatment-efficiency-and-innovation/ (accessed on 2 August 2025).

33. Hodges, B.C.; Cates, E.L.; Kim, J.-H. Challenges and Prospects of Advanced Oxidation Water Treatment Processes Using Catalytic Nanomaterials. *Nat. Nanotechnol.* **2018**, *13*, 642–650, doi:10.1038/s41565-018-0216-x.

34. Cates, E.L. Photocatalytic Water Treatment: So Where Are We Going with This? *Environ. Sci. Technol.* **2017**, *51*, 757–758, doi:10.1021/acs.est.6b06035.

35. Benotti, M.J.; Stanford, B.D.; Wert, E.C.; Snyder, S.A. Evaluation of a Photocatalytic Reactor Membrane Pilot System for the Removal of Pharmaceuticals and Endocrine Disrupting Compounds from Water. *Water Res.* **2009**, *43*, 1513–1522, doi:http://dx.doi.org/10.1016/j.watres.2008.12.049.

36. Trojan UV Resources Environmental Contaminant Treatment Product Brochure Available online: https://www.trojanuv.com/resources//Products/TrojanUVPhox/TrojanUV_ECT_Products_Brochure.pdf (accessed on 7 February 2025).

37. Rytwo, G.; Klein, T.; Margalit, S.; Mor, O.; Naftaly, A.; Daskal, G. A Continuous-Flow Device for Photocatalytic Degradation and Full Mineralization of Priority Pollutants in Water. *Desalin. Water Treat.* **2015**, *57*, 16424–16434, doi:10.1080/19443994.2015.1077749.

38. Rytwo, G.; Daskal, G. A System for Treatment of Polluted Effluents. PCT/IL2015/050944, WO2016042558 A1 2016.

39. Ishii, E.; Watanabe, Y.; Agusa, T.; Hosono, T.; Nakata, H. Acesulfame as a Suitable Sewer Tracer on Groundwater Pollution: A Case Study before and after the 2016 Mw 7.0 Kumamoto Earthquakes. *Sci. Total Environ.* **2021**, *754*, 142409, doi:10.1016/J.SCITOTENV.2020.142409.

40. Li, S.; Ren, Y.; Fu, Y.; Gao, X.; Jiang, C.; Wu, G.; Ren, H.; Geng, J. Fate of Artificial Sweeteners through Wastewater Treatment Plants and Water Treatment Processes. *PLoS One* **2018**, *13*, e0189867, doi:10.1371/journal.pone.0189867.

41. Giannakis, S.; Jovic, M.; Gasilova, N.; Pastor Gelabert, M.; Schindelholz, S.; Furbringer, J.-M.; Girault, H.; Pulgarin, C. Iohexol Degradation in Wastewater and Urine by UV-Based Advanced Oxidation Processes (AOPs): Process Modeling and by-Products Identification. *J. Environ. Manage.* **2017**, *195*, 174–185, doi:10.1016/J.JENVMAN.2016.07.004.

42. Chèvre, N. Pharmaceuticals in Surface Waters: Sources, Behavior, Ecological Risk, and Possible Solutions. Case Study of Lake Geneva, Switzerland. *Wiley Interdiscip. Rev. Water* **2014**, *1*, 69–86, doi:10.1002/wat2.1006.

43. Hrkal, Z.; Adomat, Y.; Rozman, D.; Grischek, T. Efficiency of Micropollutant Removal through Artificial Recharge and Riverbank Filtration: Case Studies of Káraný, Czech Republic and Dresden-Hosterwitz, Germany. *Environ. Earth Sci.* **2023**, *82*, doi:10.1007/s12665-023-10785-7.

44. Wang, Z.; Nguyen Song Thuy Thuy, G.; Srivastava, V.; Ambat, I.; Sillanpää, M. Photocatalytic Degradation of an Artificial Sweetener (Acesulfame-K) from Synthetic Wastewater under UV-LED Controlled Illumination. *Process Saf. Environ. Prot.* **2019**, *123*, 206–214, doi:10.1016/J.PSEP.2019.01.018.

45. Xue, H.; Gao, S.; Li, M.; Wang, Y.; Liu, B. Performance of Ultraviolet/Persulfate Process in Degrading Artificial Sweetener Acesulfame. *Environ. Res.* **2020**, *188*, 109804, doi:10.1016/J.ENVRES.2020.109804.

46. Ji, H.; Park, J.; An, S.; Choi, S.-Y.; Choe, J.K. Formation Dynamics of Inorganic Iodine Species during UV-Based Advanced Oxidation of Iopamidol and Iohexol and Their Correlation with Iodinated Disinfection by-Product Yields. *Environ. Sci. Water Res. Technol.* **2025**, doi:10.1039/D5EW00393H.

47. Perkola, N.; Vaalgamaa, S.; Jernberg, J.; Vähätalo, A. V. Degradation of Artificial Sweeteners via Direct and Indirect Photochemical Reactions. *Environ. Sci. Pollut. Res.* **2016**, *23*, 13288–13297, doi:10.1007/S11356-016-6489-4/FIGURES/4.

48. Rytwo, G.; Zelkind, A.L. Evaluation of Kinetic Pseudo-Order in the Photocatalytic Degradation of Ofloxacin. *Catalysts* **2022**, *12*, 24, doi:10.3390/catal12010024.

49. Vogna, D.; Marotta, R.; Andreozzi, R.; Napolitano, A.; D'Ischia, M.; d'Ischia, M. Kinetic and Chemical Assessment of the UV/H2O2 Treatment of Antiepileptic Drug Carbamazepine. *Chemosphere* **2004**, *54*, 497–505, doi:10.1016/S0045-6535(03)00757-4.

50. Huang, X.; Lu, G.; Zhu, X.; Pu, C.; Guo, J.; Liang, X. Insight into the Generation of Toxic By-Products during UV/H2O2 Degradation of Carbamazepine: Mechanisms, N-Transformation and Toxicity. *Chemosphere* **2024**, *358*, 142175, doi:10.1016/J.CHEMOSPHERE.2024.142175.

51. Haroune, L.; Salaun, M.; Ménard, A.; Legault, C.Y.; Bellenger, J.P. Photocatalytic Degradation of Carbamazepine and Three Derivatives Using TiO2 and ZnO: Effect of PH, Ionic Strength, and Natural Organic Matter. *Sci. Total Environ.* **2014**, *475*, 16–22, doi:10.1016/j.scitotenv.2013.12.104.

52. Chong, M.N.; Jin, B.; Laera, G.; Saint, C.P. Evaluating the Photodegradation of Carbamazepine in a Sequential Batch Photoreactor System: Impacts of Effluent Organic Matter and Inorganic Ions. *Chem. Eng. J.* **2011**, *174*, 595–602, doi:10.1016/j.cej.2011.09.065.

53. Ghosh, M.; Chowdhury, P.; Ray, A.K. Study of Solar Photocatalytic Degradation of Acesulfame K to Limit the Outpouring of Artificial Sweeteners. *Sep. Purif. Technol.* **2018**, *207*, 51–57, doi:10.1016/J.SEPPUR.2018.05.062.

54. Li, S.; Geng, J.; Wu, G.; Gao, X.; Fu, Y.; Ren, H. Removal of Artificial Sweeteners and Their Effects on Microbial Communities in Sequencing Batch Reactors. *Sci. Rep.* **2018**, *8*, 3399, doi:10.1038/s41598-018-21564-x.

55. Zilberman, A.; Gozlan, I.; Avisar, D. Pharmaceutical Transformation Products Formed by Ozonation—Does Degradation Occur? *Molecules* **2023**, *28*, 1227, doi:10.3390/MOLECULES28031227/S1.

56. Li, H.; Li, Y.; Wang, C.; Han, C.; Xu, K.; Zhang, Z.; Zhong, Q.; Shi, K.; Xu, Z.; Yang, S.; et al. Improved Degradation of Iohexol Using Electro-Enhanced Activation of Persulfate by a CuxO-Loaded Carbon Felt with Carbon Nanotubes as an Interlayer. *Sep. Purif. Technol.* **2023**, *312*, 123336, doi:10.1016/J.SEPPUR.2023.123336.

57. Hu, C.Y.; Hou, Y.Z.; Lin, Y.L.; Deng, Y.G.; Hua, S.J.; Du, Y.F.; Chen, C.W.; Wu, C.H. Kinetics and Model Development of Iohexol Degradation during UV/H2O2 and UV/S2O82− Oxidation. *Chemosphere* **2019**, *229*, 602–610, doi:10.1016/J.CHEMOSPHERE.2019.05.012.

58. Xu, M.Y.; Zeng, C.; Lin, Y.L.; Zhang, T.Y.; Fu, Q.; Zhao, H.X.; Luo, Z.N.; Zheng, Z.X.; Cao, T.C.; Hu, C.Y.; et al. Wavelength Dependency and Photosensitizer Effects in UV-LED Photodegradation of Iohexol. *Water Res.* **2024**, *255*, 121477, doi:10.1016/J.WATRES.2024.121477.

59. MRC PP-X-575PP-X-575, Basic Speed –Variable Peristaltic Pump Available online: https://www.mrclab.co.il/Media/Doc/PP-X-575-V2_SPEC.pdf.

60. NUF Technology Overview Available online: https://www.nufiltration.com/technology.

61. White, D.P. Chapter 14- Chemical Kinetics Available online: my.ilstu.edu/~ccmclau/che141/materials/outlines/chapter14.ppt.

62. IUPAC Compendium of Chemical Terminology: Gold Book. *IUPAC Compend. Chem. Terminol.* **2014**, 1670, doi:10.1351/goldbook.

63. Shahar, Y.; Rytwo, G. Elementary Steps in Steady State Kinetic Model Approximation for the Homo-Heterogeneous Photocatalysis of Carbamazepine. **2023**, *5*, 866–880.

64. Tran, H.D.; Nguyen, D.Q.; Do, P.T.; Tran, U.N.P. Kinetics of Photocatalytic Degradation of Organic Compounds: A Mini-Review and New Approach. *RSC Adv.* **2023**, *13*, 16915–16925, doi:10.1039/D3RA01970E.

65. Eddy, N.O.; Ukpe, R.A.; Ameh, P.; Ogbodo, R.; Garg, R.; Garg, R. Theoretical and Experimental Studies on Photocatalytic Removal of Methylene Blue (MetB) from Aqueous Solution Using Oyster Shell Synthesized CaO Nanoparticles (CaONP-O). *Environ. Sci. Pollut. Res.* **2023**, *30*, 81417–81432, doi:10.1007/S11356-022-22747-W/TABLES/5.

66. Mekorot Shafdan Wastewater Treatment Plant Available online: https://www.mekorot-int.com/blog/project/shepdan/ (accessed on 7 July 2025).

67. Elkayam, R.; Lev, O.; Negev, I.; Sued, O.; Shtrasler, L.; Vaizel-Ohayon, D.; Katz, Y. Soil Aquifer Treatment System Performance: Israel's Shafdan Reclamation System as an Ultimate Case Study. **2021**, 241–272, doi:10.1007/978-3-030-51148-7_14.

68. Elkayam, R.; Sopliniak, A.; Gasser, G.; Pankratov, I.; Lev, O.; Pankratov, I.; Zone, V. Oxidizer Demand in the Unsaturated Zone of a Surface-Spreading Soil Aquifer Treatment System. *Vadose Zo. J.* **2015**, *14*, 1–10, doi:10.2136/VZJ2015.03.0047.